Organic spin valves with inelastic tunneling characteristics

Kai-Shin Li,[1] Yin-Ming Chang,[1] Santhanam Agilan,[1] Jhen-Yong Hong,[1] Jung-Chi Tai,[1] Wen-Chung Chiang,[3] Keisuke Fukutani,[4] P. A. Dowben,[4] and Minn-Tsong Lin[1,2,*]

[1]*Department of Physics, National Taiwan University, Taipei 10617, Taiwan*

[2]*Institute of Atomic and Molecular Sciences Academia Sinica, Taipei 10617, Taiwan*

[3]*Department of Physics, Chinese Culture University, Taipei 11114, Taiwan*

[4]*Department of Physics and Astronomy, Nebraska Center for Materials and Nanoscience, University of Nebraska, P.O. Box 880299, Lincoln, Nebraska 68588-0299, USA*

(Received 6 September 2010; revised manuscript received 12 January 2011; published 18 May 2011)

Electrons may experience inelastic coupling with the organic spacer layer during tunneling between two ferromagnetic electrodes. To probe the transport behavior of spin-polarized electrons in organic materials, organic spin valves were fabricated utilizing a relatively thin organic barrier of 3,4,9,10-perylene-teracarboxylic dianhydride (PTCDA) dusted with alumina at the organic/ferromagnetic interfaces. These structures, with an organic barrier layer, exhibited magnetoresistance up to 12% at room temperature. In studies of the inelastic tunneling spectrum, the observed characteristic peak of the organic layer provides direct evidence of the interplay between the spin-polarized electrons and the organic molecules. Combining the inelastic tunneling results with a simple molecular vibration calculation yields further information on the configuration of the molecular thin film and the possible tunneling states of the spin-polarized electrons. Such interplay indicates a true transport of spin-polarized electrons through organic material rather than through defects or interdiffusion compounds formed at the interfaces within the organic spin valve.

DOI: 10.1103/PhysRevB.83.172404 PACS number(s): 75.47.De, 85.75.−d, 72.25.Hg, 72.80.Le

Recently, π-conjugated organic semiconductors (OSCs) have been a focus of attention in spintronics due to their potential for retaining high interface polarization values,[1] which would greatly increase the versatility of spintronic devices. By virtue of their weak spin-orbital coupling and/or long spin relaxation time, OSC materials are promising alternatives to conventional spintronic materials, and the pursuit of such an approach has helped launch and sustain the field called organic spintronics. Fabrication and investigation of organic spintronic devices such as spin valves with organic spacer layers not only provides a fundamental understanding of the transport properties of spin-polarized charge carriers in organic materials but also gives rise to potential applications, e.g., display information and flexible electronics. The rich physics involved in spin-dependent phenomena, such as the prolonged spin relaxation time and spin diffusion length found in OSC-based spin valves, is of particular interest from the view of fundamental research.[2–6] While the initial organic spin valves that achieved measurable magnetoresistance (MR) used a thick tris 8-hydroxyquinolinato aluminum (Alq_3) layer ($\geqslant$100 nm)[2], other organic layers have also been exploited.[1] Stacking a vertical structure with an organic layer in the middle is technically challenging, with issues ranging from whether growth is homogeneous, to interface abruptness and compatibility of the organic thin film with the neighboring materials, etc.[7–9] Thickness reduction of the organic layer often leads to an ill-defined organic barrier layer due to defects and poor interface quality caused by interdiffusion magnetic impurities, and pinholes. Recently, a number of groups have attempted to insert thin insulating layers (e.g., MgO and Al_2O_3) between the organic and the ferromagnetic layers to improve the spin injection efficiency.[6,10,11] But such insulating layers could become effective tunneling barriers and give rise to a measurable MR. The identification of the spin transport mechanisms through the organic layer remains an open question and is a central issue to understanding organic spintronic devices.[1]

In this work, we report the study of organic spin valves that achieve an MR ratio of ∼20% at 20 K by using a thin layer (1.25 nm) of 3,4,9,10-perylene-teracarboxylic dianhydride (PTCDA). This material has successfully been used in organic thin-film transistors and organic light-emitting diodes with good planar adhesion and exhibits small roughness on chosen substrates.[12] The organic spin valves are verified to be pinhole-free through the temperature and the PTCDA-thickness dependence of the electrical (current) characteristics. Inelastic electron tunneling spectroscopy (IETS) was used to analyze the quality and the orientation of the molecular thin films through electron-vibron interactions.[13,14] The IETS spectrum acquired from the organic spin valve structures indicates the impact of specific electron-vibronic coupling on the transport properties of the organic layer. Model calculations suggest that the molecular vibrational states are most likely of b_{2g} symmetry and are coupled to the electron tunneling states of the same symmetry (symmetric with respect to the axis defined by the interface normal). The observed inelastic characteristic provides a better picture of transport through the organic spacer layer.

The structure of our PTCDA organic spin valves was designed in the following layer sequence: NiFe (25 nm)/CoFe (15 nm)/Al_xO (0.6 nm)/PTCDA(t_P, in nm)/Al_xO (0.6 nm)/CoFe (30 nm), all deposited onto a glass substrate. A number of structures were compared that were identical apart from varying PTCDA layer thickness t_P. The whole stack was prepared in a high-vacuum environment with a base pressure of lower 10^{-8} mbar. All metallic layers were made by sputtering with an Ar working pressure of 5×10^{-3} mbar whereas the PTCDA layers were grown by thermal evaporation at 10^{-8} mbar, with a deposition rate of 0.1 nm/s. At the interface between the organic PTCDA layer and the ferromagnetic layer of either side, a thin Al_xO layer was made by partially oxidizing an aluminum layer in an oxygen plasma for 5 s.[6,13,15] As is well known, metals are prone

to react with the anhydride (C-O) end groups of PTCDA, resulting in the formation of a mixed oxidation layer.[16] The Al_xO layer suppressed formation of such a hybrid layer or pinholes at the interface with both CoFe layers. A slightly oxidized Al layer has been suggested to be an effective way to isolate interface effects which might otherwise reduce the electron injection efficiency and the spin polarization of the ferromagnetic layer and to retain the spin polarization in these organic spin valves with the large-scale junction areas.[6] This approach should not be overgeneralized. As indicated by a recent study on a Co/Alq_3/LaSrMnO nano-pore device,[17] many physical parameters, such as junction area, the functional groups of molecule, and the fabrication conditions of the spin valve device, can all influence the spin polarization of the interface hybrid state. With a well-controlled interface between a ferromagnet and a molecule, the intrinsic spin interface effects might also lead to enhanced values of interface spin-polarization.[18,19] The spin valves were patterned *in situ* with a sequence of shadow masks and the junction area, measured to be 200 × 200 μm, was defined by the intersection of the crossed electrodes. The resistance measurements were carried out by the conventional four-point probe methods in a controlled temperature-varying environment.

The room-temperature MR curves for a series of hybrid PTCDA-based spin valves, with various barrier thicknesses t_P, are illustrated in Fig. 1. An MR ratio of ~12% is observed with 1.25-nm PTCDA. Fluctuations in the coercivity of the top electrode were observed with changing PTCDA thickness t_P. The magnetic properties, as well as the interfacial spin-polarization of ferromagnetic materials, are very sensitive to the surface quality and roughness of the underlayers, particularly at the nanometer scale.[20] Since the growth and the surface structure of the organic layer can be strongly dependent on thickness, the magnetic behavior of the upper magnetic layer can also be significantly affected.[21] As the PTCDA layer thickness increased, the magnitude of the MR ratio was observed to decrease rapidly and vanishes at or above a t_P value of 5 nm. A test device made by producing a PTCDA-empty ($t_P = 0$) sample shows zero MR—an indication that the partially oxidized Al layer alone cannot form an effective spin-transport barrier. Pinholes are likely to form with such a small amount of Al oxidization, which would decrease the MR ratio.[22] The pinhole effects are reduced by further deposition of PTCDA and a reasonable MR can thus be obtained.[23] On the other hand, Al may diffuse into the PTCDA layer, by reacting with anhydride (C-O) end groups, during deposition. The diffusion depth for Al on the PTCDA layer could reach about 2 nm.[16] As seen in the inset of Fig. 1, the slope of the junction conductance as a function of PTCDA thickness is nearly constant. This implies that such diffusion might have only a slight influence on the junction conductance of the spin valve. We speculate that the deposited 0.6-nm Al may form only a very thin Al_xO-PTCDA hybrid layer at the interface, and the variation of junction conductance for this type of organic spin valve is basically set by changing thickness of the PTCDA barrier. The inset of Fig. 1 shows that the junction conductance (G_J) scales exponentially with the PTCDA thickness, providing a clear indication that the junctions are pinhole-free and that G_J is dominated by the resistance of the PTCDA layer. An extinction coefficient of $\beta = 0.12$ Å^{-1} is obtained by fitting G_J with $G_0 e^{-\beta d}$, where G_0 is the contact conductance and d is the thin film thickness. Low β values have been reported in other π-conjugate molecules, with values ranging from 0.08 to 0.41 Å^{-1},[17,24,25] and have been attributed to the reduction of the effective barrier height due to image potential contributions or interface dipole field effects.[17]

Figure 2(a) shows the temperature dependence of the MR ratio for the sample with 1.25-nm PTCDA. The temperature

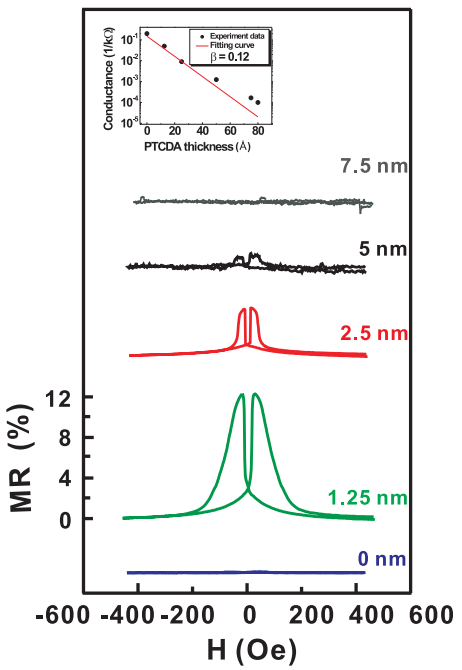

FIG. 1. (Color online) Magnetoresistance curves for a series of PTCDA-based organic spin valves with various barrier thicknesses (t_P), measured at room temperature. The PTCDA-empty ($t_P = 0$) sample exhibits no magnetoresistance. The inset plots the junction conductance (G_J) vs t_P on a logarithmic scale.

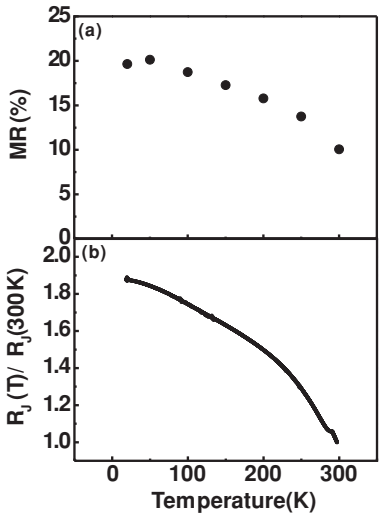

FIG. 2. (a) MR ratios for a PTCDA spin valve with $t_P = 1.25$ nm, measured at 10 mV, as a function of temperature. (b) Normalized junction resistance vs temperature for the same sample.

dependence of the junction resistance (R_J, normalized) for the same sample is given in Fig. 2(b). Upon cooling, the increase of junction resistance is substantially more dramatic than that typically seen in Al_2O_3-based tunnel junctions. A similar phenomenon has been reported in disordered organic thin film junctions and is thought to originate from inelastic transport via localized states (defects, impurities, etc.) in the organic barrier.[13,14] The MR ratio increases by a factor of ~2 when the temperature is reduced from 300 to 20 K. The increase is also more substantial than that of ordinary tunnel junctions, which, in principle, should show little temperature dependence well below the Curie temperature. The strong temperature dependence of MR ratio is seen in LaSrMnO-electrode systems but the magnetization is highly temperature dependent in these systems.[15] In metallic-electrode systems of high Curie temperature ferromagnetic 3*d* metals and alloys (e.g., Co, Fe, and CoFe), the same mechanism is not likely to account for the extraordinary increase of MR. From the large enhancement of R_J in Fig. 2(b), we postulate that the enhanced temperature dependence of the MR ratio observed in our PTCDA-based spin valves could be due to spin scattering in the high-temperature regime. This is not unreasonable as spin scattering (or inelastic transport) in organic systems is seen to be significantly dependent on temperature, thus affecting coherent spin transport.[26]

To probe the electron coupling to the molecular vibrational modes within the PTCDA spin valve, IETS was conducted on the organic junctions at 20 K. The first- and second-derivative *I*-*V* characteristics have been measured and plotted in the top and the bottom plots of Fig. 3(a), respectively. The spectra are reproducible upon successive bias sweeps, with one pronounced vibronic loss peak detected at 46.7 mV within the range of 0–100 mV. With a Al_2O_3-barrier junction, only two peaks at 110 and 450 mV are present in the IETS spectrum,[27] corresponding to the Al-O stretching mode and the surface OH^- stretching mode. The magnon excitation in magnetic tunnel junctions has also been observed by the IETS peaking at 17 mV, causing the zero bias anomaly MR.[28] All of those IETS peaks are far from the vibronic loss peak position (47 mV) we observe. This result is, however, consistent with the previously reported IETS scanning tunneling microscope data of adsorbed PTCDA molecules.[29] This signature of a PTCDA vibronic loss, when combined with the aforementioned $I(V)$ characteristics, is a strong indication that the rise of magnetoresistance is indeed mediated by the spin carriers across the PTCDA layer. The line shape of the 46.7-mV peak could be due to the different resonance energies, as suggested by Galperin *et al.*[30] and Mii *et al.*[31] Figure 3(b) shows the second-derivative IETS spectra taken at various temperatures. The peak exhibits the typical thermal broadening effect of IETS and vanishes when temperature is elevated above 100 K.

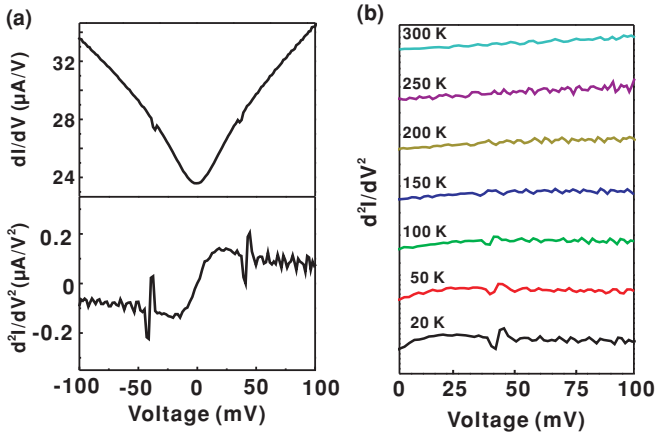

FIG. 3. (Color online) (a) First-derivative (top) and second-derivative (bottom) IETS spectra for a PTCDA spin valve with $t_P = 1.25$ nm, measured at 20 K. A pronounced peak is detected at 46.7 mV. (b) Second-derivative IETS spectra for the same sample measured at various temperatures.

To further investigate the vibrational modes of PTCDA molecule, we used SPARTAN software to perform density functional theory (DFT) calculations, which are based on the density functional formalism (B3LYP) using a harmonic oscillator potential and the extended basis set 6-31G* to obtain the dipole-active modes (IR-like), as well as all the vibrational modes for a free molecule. Figure 4(a) shows the resulting eigenvalues of the vibrational modes for the PTCDA molecule with each key mode labeled by a number and a diagram.

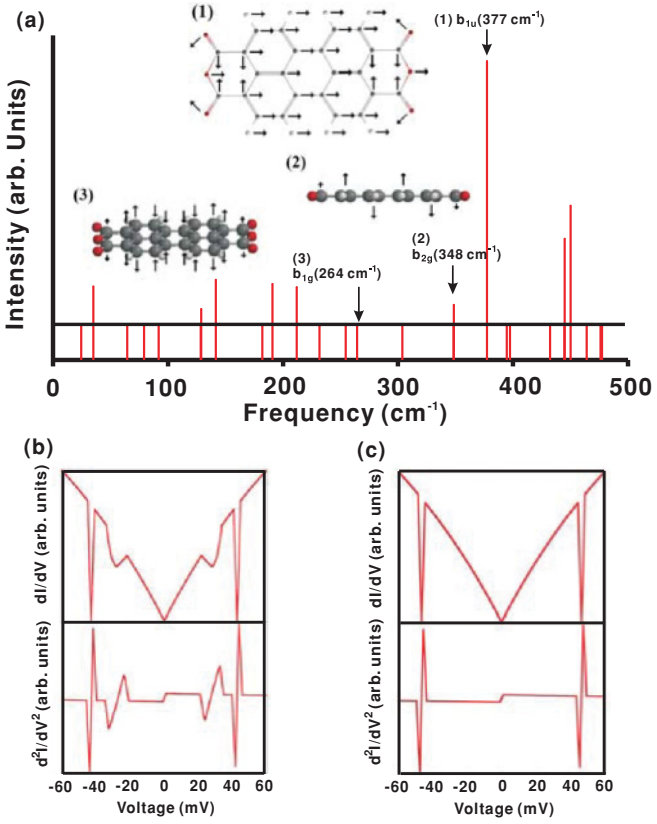

FIG. 4. (Color online) (a) The vibrational modes of the PTCDA molecule, obtained from a DFT calculation, in which (1) the in-plane (377 cm^{-1}) and (2) the out-of-plane (348 cm^{-1}) modes are dipole-active, whereas (3) the twisting (264 cm^{-1}) mode is dipole-active when PTCDA grows on the conducting substrate. The arrows in the molecular description indicate the relative motion of each atom. (b) The peaks of simulated conductivity and the IETS spectrum in a PTCDA thin film with planar configuration are from (2) the out-of-plane vibrational mode (42 mV), from (3) the twisting vibrational mode (34 mV), and (c) from (1) the in-plane vibrational mode (47 mV) with upright configuration.

(1) (377 cm^{-1}) indicates the top view of this pure in-plane mode, (2) (348 cm^{-1}) indicates the side view of this out-of-plane mode, and (3) (264 cm^{-1}) indicates the 45° view of this out-of-plane "twisting" mode. Combining DFT and the Simmons model[32] in the calculation of tunneling spectra leads to a simulation of IETS, with PTCDA lying in a planar configuration [shown in Fig. 4(b)] and placed in an upright configuration [shown in Fig. 4(c)] in which we assume that the conduction is dominated by s, p_z, and d_{z^2} electron states. The transport electron wave function may still preserve symmetry character after passing through the slightly oxidized Al to the PTCDA layer.

The theory provides information on the symmetry character of the wave functions involved in the electron transport. The symmetry restrictions of the available vibrational modes suggest that when PTCDA lies in-plane, inelastic tunneling in our structure is dominated by the d_{xy}, d_{xz}, p_x, and p_y symmetry wave functions originated from the electrodes rather than the s or the d_{z^2} symmetry function. On the other hand, if PTCDA aligns upright to the substrate plane, then inelastic tunneling could well occur though the d_{z^2} and s frontier orbitals of the electrodes. Consequently, the experimental data in Fig. 3(a) are determined by the molecular configuration of the PTCDA thin film, which means the peak of the IETS spectrum in the PTCDA spin valve with a planar configuration could be contributed from (2) the out-of-plane vibrational mode (348 cm^{-1}) at ∼42 mV, (3) the twisting vibrational mode (264 cm^{-1}) at ∼34 mV, or (1) the in-plane vibrational mode (348 cm^{-1}) at ∼47 mV with upright configuration. Vibrational modes like the mode at 264 cm^{-1} become dipole-active if the PTCDA thin film is intimately connected to a conducting substrate. In our system, PTCDA is laid on a thin Al_xO layer; therefore the only observable mode would be either the in-plane (377 cm^{-1}) or the out-of-plane (348 cm^{-1}) mode depending on the orientation and the dominant symmetry of the conduction electron states. Previous studies have shown that PTCDA tends to be aligned nearly in-plane with the substrate due to the layered crystalline structure and the intrinsic molecular quadrupole moment.[33] X-ray diffraction (XRD) results of our PTCDA thin films reveal only one peak ($2\theta = 27°$) corresponding to the [102] plane of the PTCDA crystalline structure, suggesting that the [102] direction is centered about 15° from the film normal. As most PTCDA molecules within the unit cell are parallel to this plane, it follows that the molecules are close to parallel to the substrate plane, with an average inclination of 10°–15°.[33] Summarizing these arguments we may conclude that most PTCDA molecules follow planar growth on the substrate, and the electron-vibron coupling observed in the IETS spectra is mainly dominated by the out-of-plane vibrational mode (348 cm^{-1}) and that the conduction state symmetry should have then significant contributions from p_x, p_y, d_{xz}, and d_{yz} states (i.e., b_{2g} symmetry states).

In conclusion, we have performed spin injection measurements in tunnel junctions containing an organic PTCDA barrier, and MR ratios of 12% and ∼20% were obtained at room temperature and 20 K, respectively. With IETS measurements, we have also demonstrated that the transport of the charge carriers couples with the molecular vibrational states. The PTCDA molecules are most likely to align flat along the substrate plane, with the electron-vibron coupling dominated by the out-of-plane vibrational mode. The electron–organic layer interplay gives insight into the transport mechanism of organic spin valves. The advantage of organic spintronics becomes more realistic when the charge carriers indeed transport through the organic layer with the imposition of organic characteristics.

*mtlin@phys.ntu.edu.tw

[1] J. P. Velev *et al.*, Surf. Sci. Rep. **63**, 400 (2008).
[2] Z. H. Xiong *et al.*, Nature (London) **427**, 821 (2004).
[3] V. Dediu *et al.*, Solid State Commun. **122**, 181 (2002).
[4] S. Pramanik *et al.*, Nature Nanotech. **2**, 216 (2007).
[5] Y. Q. Zhan *et al.*, Phys. Rev. B **78**, 045208 (2008).
[6] T. S. Santos *et al.*, Phys. Rev. Lett. **98**, 016601 (2007).
[7] W. Xu *et al.*, Appl. Phys. Lett. **90**, 072506 (2007).
[8] H. Vinzelberg *et al.*, J. Appl. Phys. **103**, 093720 (2008).
[9] J. S. Jiang *et al.*, Phys. Rev. B **77**, 035303 (2008).
[10] G. Szulczewski *et al.*, Appl. Phys. Lett. **95**, 202506 (2009).
[11] J.-W. Yoo *et al.*, Phys. Rev. B **80**, 205207 (2009).
[12] S. Kowarik *et al.*, J. Phys. Condens. Matter **20**, 184005 (2008).
[13] J. H. Shim *et al.*, Phys. Rev. Lett. **100**, 226603 (2008).
[14] K. V. Raman *et al.*, Phys. Rev. B **80**, 195212 (2009).
[15] V. Dediu *et al.*, Phys. Rev. B **78**, 115203 (2008).
[16] Y. Hirose *et al.*, Phys. Rev. B **54**, 13748 (1996).
[17] C. Barraud *et al.*, Nature Phys. **6**, 615 (2010).
[18] S. Javaid *et al.*, Phys. Rev. Lett. **105**, 077201 (2010).
[19] S. Schmaus *et al.*, Nature Nanotech. **6**, 185 (2011).
[20] J. C. Tai *et al.*, Appl. Phys. Lett. **96**, 262502 (2010).
[21] M. V. Tiba *et al.*, AIP Conf. Proc. **696**, 521 (2003).
[22] D. Song *et al.*, J. Appl. Phys. **87**, 5197 (2000).
[23] J.-W. Yoo *et al.*, Nature Mater. **9**, 638 (2010).
[24] T. Tada *et al.*, J. Am. Chem. Soc. **126**, 14182 (2004).
[25] M. Magoga and C. Joachim, Phys. Rev. B **56**, 4722 (1997).
[26] C. H. Shang *et al.*, Phys. Rev. B **58**, R2917 (1998).
[27] E. L. Wolf, *Principles of Electron Tunneling Spectroscopy* (Oxford University Press, New York, 1985).
[28] J. S. Moodera *et al.*, Phys. Rev. Lett. **80**, 2941 (1998).
[29] R. Temirov *et al.*, J. Phys. Condens. Matter **20**, 224010 (2008).
[30] M. Galperin *et al.*, Nano Lett. **4**, 1605 (2004).
[31] T. Mii *et al.*, Phys. Rev. B **68**, 205406 (2003).
[32] J. G. Simmons, J. Appl. Phys. **34**, 1793 (1963).
[33] A. J. Lovinger *et al.*, J. Appl. Phys. **55**, 473 (1984).